

Crafting Parts for Expressive Object Composition

Harsh Rangwani^{1,2}, Aishwarya Agarwal², Kuldeep Kulkarni², R. Venkatesh Babu¹, and Srikrishna Karanam²

¹ Indian Institute of Science

² Adobe Research, Bengaluru India
harshr@iisc.ac.in

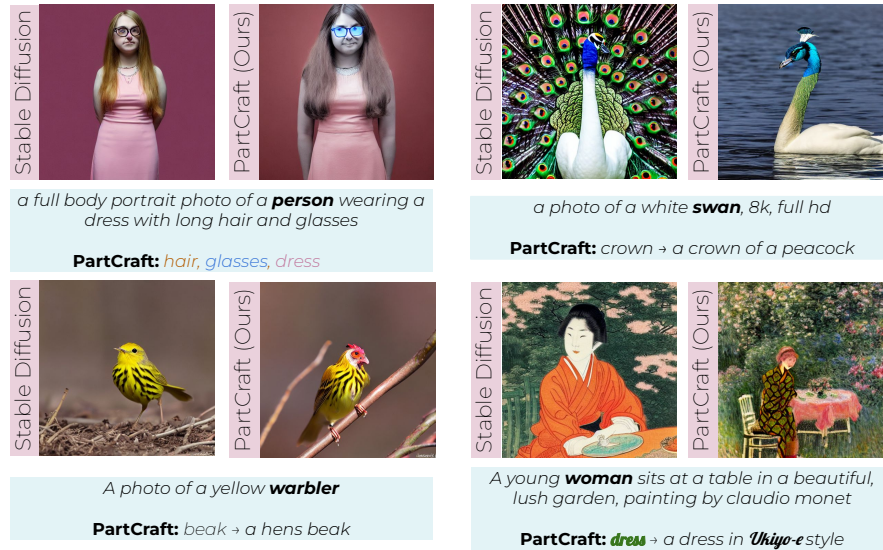


Fig. 1: Stable Diffusion vs PartCraft (Ours). PartCraft allows the generation of object images with specified attributes (color, style *etc.*) of parts for the **chosen object** in the text prompt. The StableDiffusion baseline generations (left) with part details added to prompt lead to inconsistent outputs compared to proposed PartCraft.

Abstract. Text-to-image generation from large generative models like Stable Diffusion, DALLE-2, etc., have become a common base for various tasks due to their superior quality and extensive knowledge bases. As image composition and generation are creative processes where the artists need control over various parts of the images being generated. We find that just adding details about parts in the base text prompt either leads to an entirely different image (e.g., missing/incorrect identity) or the extra part details simply being ignored. To mitigate these issues, we introduce PartCraft, which enables image generation based on fine-grained part-level details specified for objects in the base text prompt. This allows more control for artists and enables novel object compositions by combining distinctive object parts. PartCraft first localizes object parts by denoising the object region from a specific diffusion process. This enables each part token to be localized to the right object region. After obtaining part

masks, we run a localized diffusion process in each of the part regions based on fine-grained part descriptions and combine them to produce the final image. All the stages of PartCraft are based on repurposing a pre-trained diffusion model, which enables it to generalize across various domains without training. We demonstrate the effectiveness of part-level control provided by PartCraft qualitatively through visual examples and quantitatively in comparison to the contemporary baselines.¹

1 Introduction

Image generation with large generative diffusion models like StableDiffusion [29], DALLE [28], etc., has become prevalent due to their superior quality and extensive knowledge bases. These models are trained on large image-caption datasets and are trained to generate images based on a given text prompt (description). As image composition and creation are creative processes where the artists need control over various parts of the image being generated. However, adding additional details about parts in the text prompt either changes the entire image composition for text-to-image models or ignores the artist’s instructions [8] (warbler in Fig. 1).

There are various works that aim to provide spatial controls to image generation, they allow image generation conditioned on segmentation masks [4], edge maps [41], bounding boxes [9, 22] etc. Popular methods such as ControlNet [41], GLIGEN [22], etc. require specifying training of these conditional modules, which allows for the controllability of these large generative models. Further, there has been some development of training-free approaches [8, 9] which enable controlled generation of objects by modulating the internal cross-attention activations in the diffusion process. This demonstrates that these pre-trained generative models contain information about the spatial parts of the image, and modulating them effectively can lead to effective image compositions.

However, despite the plethora of works focusing on controllability, the semantic controllability of the image generation is still restricted to specifying details at the object level. The object level details can be restrictive, as often creative designers synthesize object parts (*e.g.* shirt, trouser etc.) and then compose them [19]. Further, variations in semantic parts are often very distinctive and are used to identify objects [11, 24] uniquely. For example, we usually identify species of birds by their unique *beak*. Due to this, semantic understanding and recognition of parts have been widely studied as a topic in computer vision [11, 12, 17, 25]. Hence, providing controllability for image synthesis at the object semantic part level can enable a large variety of image compositions [19]. Towards this goal, we introduce **PartCraft** which provides users with an interface, through which they can select the object in the scene and provide a semantic part-level description with fine-grained details for the object generation .

In **PartCraft** we first develop a scheme to extract part-level segmentation masks from the StableDiffusion model. For this, we introduce a parallel part diffusion process that generates masks for the object parts. The core idea of

¹ Project Page: <https://rangwani-harsh.github.io/PartCraft>

the approach is that by forcing the part diffusion model to specifically denoise only the object region in the image, it is possible to get an understanding of the locations of various parts in the object. After composing the object through the part model, the information inside the part diffusion model present in attention maps can be used to generate the masks for various object parts. In the second part, PartCraft utilizes the part masks and description of each part provided by the user. We enable users to provide a highly expressive specification of parts by using a Rich-Text [14] interface, which allows specifying of various styles, colors, etc. for each of the parts.

For generating the final image, taking inspiration from recent studies like Rich-Text Generation [14], Multi-Diffusion [4] etc. we compose the various object parts, by running parallel masked diffusion process for each part while combining them periodically. This combination enables harmonious composition of parts and also makes sure to only locally modify the region corresponding to each part of the object specified by part masks. In the PartCraft pipeline we only make use of the pre-trained StableDiffusion model, and don't perform any kind of training.

We extensively test proposed PartCraft approach for the zero-shot object part segmentation, which is a very challenging setup in computer vision. We evaluate the part segmentation approach on DeepFashion [23] and CUB200 [38] datasets, where our method significantly outperforms in the baseline StableDiffusion. Further, to evaluate the PartCraft image composition process, we also provide quantitative and user study results, where our method significantly outperformed the baselines in generating consistent images composed of the described parts Fig. 1. We summarize the core contributions of our paper below:

1. We introduce PartCraft, a training-free method that enables the generation of object images by providing fine-grained details for the parts of the object. For example, for a bird we can specify a distinctive description of its beak.
2. In PartCraft, we introduce a novel Part-Diffusion process, which localizes and provides masks for object parts, for objects generated by the Base Diffusion model (Fig. 3). To localize object parts, we introduce a segmentation scheme that makes use of the attention maps of the base diffusion and part diffusion process to obtain accurate masks for localized parts .
3. In PartCraft after localization, we enable the generation of parts from the pre-trained diffusion model based on the Rich-Text description for the parts provided by the user. PartCraft then composes the image such that all object parts are harmoniously blended by combining localized diffusion path (Fig. 2).

2 Related Works

Text-2-Image Generative Models. The text-2-image models aim at synthesizing images by following a textual description provided as a prompt. These models have recently become mainstream due to their superior quality and significant knowledge base. This is an outcome of the availability of large-scale image caption datasets [30] and highly parallelized GPU clusters. Almost all kinds of generative

models, such as GANs [18], Autoregressive [40], and Diffusion models [28, 29], have shown significant improvements in quality due to training on these large image caption datasets. Among these models, the StableDiffusion [29] models which are based on Diffusion in Latent space are popular due to their open-source nature, which we also utilize for experiments in our work.

Text-2-Image Models for Downstream Tasks. Generative models, in general, have been useful for various downstream tasks, particularly ones based on per-pixel prediction like Segmentation [1, 10], Depth Estimation [6], etc. As layers near the image generation output have features that capture the pixel-pixel relation [6]. With the large-scale text-2-image generative models, these models often perform very competitively [34, 39] to discriminative methods, on tasks like segmentation. However, one commonality among most of these segmentation methods is that they operate at granularity of object or instance level. Text-2-image models here are at an advantage as the usual image captions describe the scene at an object level. In this work, we take a step further exploring the object part level knowledge of these text-2-image diffusion models.

Part Discovery and Segmentation. Part Discovery and Attribution were an integral part of computer vision pipelines classically, as these approaches were robust to view point variations [20, 25, 36]. In deep learning, the unsupervised (self-supervised) approaches for part discovery like SCOPS [17] and Unsup-Parts [11] became popular as they generalize to object parts across categories. In this work, we go one step ahead and operate in zero shot unsupervised part segmentation, where we generate part masks from large Text-2-Image diffusion models.

Controllable Image Generation. Masks along with bounding boxes, edge maps, depth maps etc. have been explored to control the generations of text-2-image diffusion models [5, 22, 41] in addition to text. Further, various other approaches [2, 3, 8, 33, 37] achieve control of image semantics, through modulating diffusion models. Despite this the text-2-image generation control at object part level is unexplored, which we do in our work PartCraft.

3 PartCraft

In this section, we introduce PartCraft, the method to synthesize objects based on the description of parts of the objects. In PartCraft, we ask the user to specify a base prompt and the token for the object it wants to synthesize parts. Then we provide a *rich-text* [14] based editor to the user to specify the parts and their description. Our work PartCraft, involves two diffusion steps. **a) Part Localization.** In the first diffusion step, we get a mask for the object we want to divide into parts. Then, we perform denoising from a U-Net condition on parts to fill the masked region of the object, during which it learns to denoise different object parts. Due to this, the attention maps for various parts start highlighting the correct part region, which we use to extract the part mask. The infilling process is the major contribution of the PartCraft method. **b) Part Generation.** For generating parts we make combine region specific diffusion

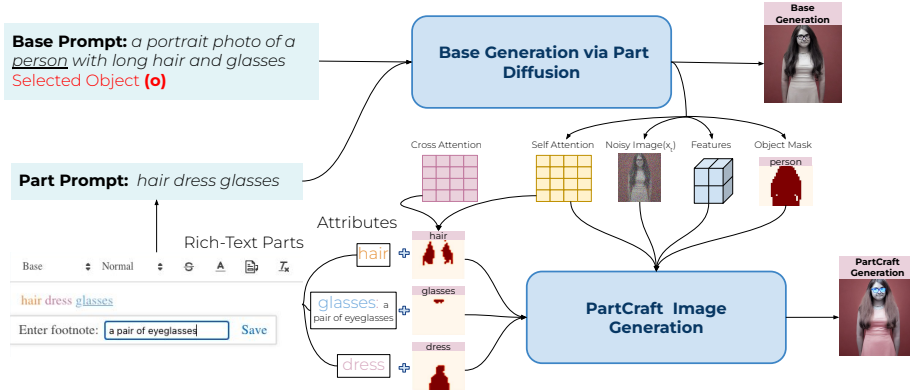


Fig. 2: PartCraft takes input: a base prompt, the selected object \mathbf{o} , and a Rich-Text description of the parts. The Part Diffusion process generates the object masks for the specified parts. Then, PartCraft runs a parallel Region Diffusion process to generate attributes of the specified parts, guided by base generation’s intermediate outputs.

process for various parts by iteratively merging them inspired by MultiDiffusion [4], Rich-Text Generation [14] etc. However, till now most of these works have combined the diffusion process for generating objects, for the first time we demonstrate it’s effectiveness in generating object parts. We provide the overview of the PartCraft Generation process in Fig. 2. We below describe the Problem setup followed by the Part Generation and Part Localization setups in detail.

3.1 Problem Setup

We consider each span of tokens \mathbf{p}_i as indicative of describing one part of the object, with attributes \mathbf{a}_i describing in appearance. The users are provided with the following ways to describe the parts in terms of their attributes \mathbf{a}_i of the object. Our design choices are based on the rich-text generation [14], which allows us to explore various controls for part generation. The

Part Description. The part description (*i.e.* footnote) is an important attribute that specifies the part of an object; for example, for the part (\mathbf{p}_i) ‘crown’ of a bird, we can specify the attribute ($\mathbf{a}_i^p = \text{‘a crown of a peacock’}$). This helps in specifying novel part descriptions, which can lead to artistic novel compositions.

Font Color. The font color helps us specify the exact RGB values for the color attribute \mathbf{a}_i^c , we want for the object part \mathbf{p}_i . The exact value of RGB allows fine grained control over color of the desired part, whereby just specifying specific colors like ‘brick red’ lead to ignorance by Stable Diffusion [14].

Font Style. The font style is indicative of the specific artistic style \mathbf{a}_i^s like ‘of Claude Monet’ and ‘of Van Gogh’ when synthesizing images of paintings. This instructs the model to generate a part following a specific style for the given prompt and blend it with other parts of the object. The uniqueness of PartCraft

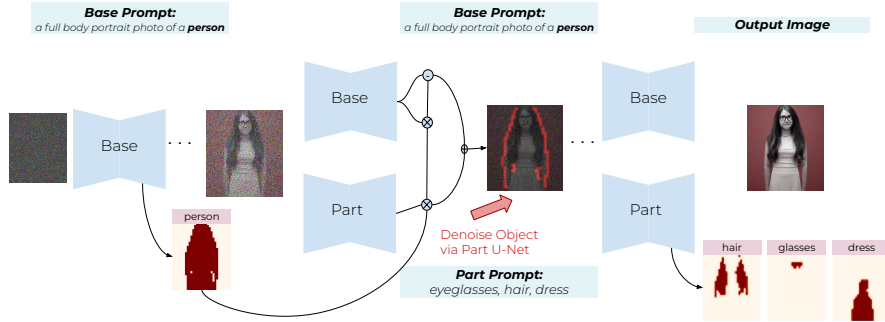


Fig. 3: Localization. We obtain the mask (\mathcal{M}_o) for object in middle of diffusion process. We then denoise object in masked region, using parts \mathbf{p}_i conditioned U-Net. Due to part denoising, the attention maps of \mathbf{p}_i can now localize parts as masks $\mathbf{M}_{\mathbf{p}_i}$.

is that it can specify part styles even for objects in paintings and comics, as it’s based on extracting knowledge from large-scale text-2-image models (Sec. 5).

Font Size. The font size controls the relative size of each part in a generation [15]. We use the \mathbf{a}_i^w to denote the size of each token.

3.2 Part Localization

We now describe our Part Denoising approach to localize various semantic parts in an object. We first run the base stable diffusion model for the given text prompt and extract the token map \mathcal{M}_o for the object \mathbf{o} specified by user, by following the technique of clustering the self-attention maps [14, 27]. We perform this operation at time t less than total time steps for the Diffusion process T . After obtaining the binary object mask \mathcal{M}_o using attention masks [14, 27], we run two parallel diffusion processes in which one contains input from the text prompt and one contains input from the part prompts $\hat{\mathbf{p}} = [\mathbf{p}_1, \mathbf{p}_2, \dots, \mathbf{p}_n]$. One token for each of the part specified in the part text prompt. We denote the $\hat{\mathbf{b}}$ to denote the base text prompt and $\hat{\mathbf{p}}$ to denote the part prompt. For the time $t \leq T_{th}$ (by default we use $T_{th} \approx T/2$) we denoise the U-Net in the object region by denoising it with both the combination of the Part prompt output and Base Prompt Output. Due to this, the Part-Based U-Net gets the information regarding various parts in the object (Fig. 3). We now mathematically define the output noise ϵ_t for the diffusion process with Part-Diffusion below:

$$\epsilon_t = \alpha * \mathcal{M}_o \odot D(x_t, \hat{\mathbf{p}}, t) + (1 - \alpha) * \mathcal{M}_o \odot D(x_t, \hat{\mathbf{b}}, t) + (1 - \mathcal{M}_o) \odot D(x_t, \hat{\mathbf{b}}, t) \quad (1)$$

here, the α is the hyper-parameter which controls the strength of the part prompt diffusion output, and D is the output of the pre-trained U-Net of a text-2-image diffusion model. On performing some algebra, the above expression can be simplified as the following:

$$\epsilon_t = \alpha * \mathcal{M}_o \odot D(x_t, \hat{\mathbf{p}}, t) + (1 - \alpha * \mathcal{M}_o) \odot D(x_t, \hat{\mathbf{b}}, t) \quad (2)$$

The above denoising process is followed for t steps till 0, to complete one denoising iteration and produce a base image that corresponds to the given prompt \hat{b} . Keeping a high T_{th} and low α , makes minimal changes in output as if the denoising diffusion was done with original prompt \hat{b} (See Supp. Sec.). With this denoising, we obtain attention masks, from which we extract the localization information of part \mathbf{p}_t . We now describe the part localization process below.

Token Maps for Parts. We first take the part tokens $\hat{\mathbf{p}}$, which are a concatenation of the part names (*e.g.* ‘beak crown wings’, etc.), which may not make a meaningful text prompt. Hence, we initialize text embeddings for all these tokens by passing the meaningful text prompt having the following template: “ A photo of \mathbf{p}_i of a \mathbf{o} ” where \mathbf{p}_i is the object part name and \mathbf{o} is the object name. This serves two purposes: first, it makes the embedding meaningful, and second, it introduces some invariance from the order of part specification in part prompt. These embeddings are then passed as text embeddings to the Part U-Net for denoising. After embedding and running the denoising process, we aggregate across heads and time the self-attention maps (from 32×32 resolution) from both the base and part U-Net diffusion, taking inspiration from works that demonstrate that attention can localize objects [8, 14, 24, 32]. We then perform spectral clustering on these attention maps to form. Based on pixel-pixel similarity, k segmentation maps $\hat{\mathbf{M}}$ (32×32). To attribute these K -segments to the part specified by the user, we aggregate the cross attention of Part U-Net diffusion process. For each token \mathbf{p}_j , we obtain the cross-attention score as follows:

$$\hat{\mathbf{m}}_j = \frac{c_j}{\sum_k c_k} \quad (3)$$

where c_j is the cross attention score for each token. We proceed by averaging the attention heads to obtain the average cross-attention scores and resize them to 32×32 obtaining $\hat{\mathbf{m}}$. We proceed by removing the start of text (<‘<not>’) token before taking the softmax for cross-attention and then re-normalize it [8]. In other works [14, 27], as the tokens correspond to the image being generated, it’s sure that token maps will be meaningful. However, for parts, it’s not true, as the Part U-Net might not localize some parts. For determining if the part is localized, *we propose to look at the max value of cross attention map spatially across the resolution*; if we find that the following condition is met, the part is localized:

$$L(j) = \mathbb{1}\{\max(\hat{\mathbf{m}}_j) \geq (1 - \delta)\frac{1}{K}\}. \quad (4)$$

Here δ is a hyperparameter, and K is the number of parts. This condition is robust in finding the localized parts (See Sec. 5 for ablation). For the parts \mathbf{p}_i , which are localized, we normalize the cross-attention map. We follow a dot-product-based protocol to assign each of the K clusters in the attention map to a part, unlike the average attention protocol in the previous works [14, 27].

$$\hat{\mathbf{m}}_j = L(j) \frac{\hat{\mathbf{m}}_j - \min(\hat{\mathbf{m}}_j)}{\max(\hat{\mathbf{m}}_j) - \min(\hat{\mathbf{m}}_j)} + (1 - L(j)) \hat{\mathbf{m}}_j \quad (5)$$

We find that dot product of normalized cross attention scores $\hat{\mathbf{m}}_j$ for each token with self-attention masks $\hat{\mathbf{M}}_j$ works better, as the attention maps in Part-Unet are noisy. Still, they are often correct for the regions which are localized in one specific area only (Refer Suppl. Sec.). Hence, the dot product protocol favors those maps that are only localized in some areas of the image and don't have high attention values across all parts of the object. After obtaining the dot product scores for each part we assign $\hat{\mathbf{M}}_j$ to \mathbf{p}_i with highest scores. The mask for the part \mathbf{p}_i is finally given as the following:

$$\mathbf{M}_{\mathbf{p}_i} = \{\cup_j \hat{\mathbf{M}}_j | \operatorname{argmax}_i \hat{\mathbf{M}}_j \cdot \hat{\mathbf{m}}_i = i \text{ and } \hat{\mathbf{M}}_j \cdot \hat{\mathbf{m}}_i \geq \epsilon, \} \quad (6)$$

Here ϵ is the hyperparameter which controls the minimum similarity required between the attention mask and the part token. We combine the additional attention masks unassigned to any token, and name them as the background (other) token \mathbf{M}_b . In the following sections, we evaluate the generated part token masks as zero-shot unsupervised part segmentation (See Fig. 4).

3.3 Part Generation

We follow a similar protocol for the generation of part segments as in Rich-Text Generation. We tailor the rich text generation to compose the part regions of the object in the image in place of the original scene composition. We describe the part generation protocol below briefly and refer readers to Rich-Text Gen [14] for more details. For each part \mathbf{p}_i we run a region diffusion process, which runs in parallel for all the parts. We then combine the region diffusion processes to obtain the final noise prediction ϵ_t as the masked $\mathbf{M}_{\mathbf{p}_i}$ sum of the denoiser outputs:

$$\epsilon_t = \sum_i \mathbf{M}_{\mathbf{p}_i} \epsilon_{t, \mathbf{p}_i} = \sum_i \mathbf{M}_{\mathbf{p}_i} \odot D(x_t, f(\mathbf{p}_i, \mathbf{a}_i), t) \quad (7)$$

where D is the pre-trained U-Net model, and $f(\mathbf{p}_i, \mathbf{a}_i)$ is the text description of the part \mathbf{p}_i constructed using the following process using the part tokens \mathbf{p}_i and attributes \mathbf{a}_i . Initially the the text $f(\mathbf{p}_i, \mathbf{a}_i) = \mathbf{p}_i$, is set to part token itself. In case the part description (i.e. footnote) is available we set the $f(\mathbf{p}_i, \mathbf{a}_i) = \mathbf{a}_i^p$, further if the style attribute is available we do $f(\mathbf{p}_i, \mathbf{a}_i) + =$ in style of $+$ \mathbf{a}_i^s . In case the color attribute is also specified, the nearest named color $\hat{\mathbf{a}}_i^c$ (e.g. red) for the specific RGB color \mathbf{a}_i^c is found, and $f(\mathbf{p}_i, \mathbf{a}_i) = \hat{\mathbf{a}}_i^c + ' ' + f(\mathbf{p}_i, \mathbf{a}_i)$. The string $f(\mathbf{p}_i, \mathbf{a}_i)$ is the text input for the Diffusion to generate the part \mathbf{p}_i . We use the base prompt $\hat{\mathbf{b}}$ as $f(\mathbf{p}_i, \mathbf{a}_i)$ for the background masked region \mathbf{M}_b . This combination of different diffusion outputs at every time t helps generate a harmonious image after composing the defined parts.

Following Rich-Text [14], we also utilize the gradient guidance [13, 16] by taking the gradient of MSE loss between the estimated original image and the color value \mathbf{a}_i^c specified by the user. The gradient guidance helps in generating exact color for part \mathbf{p}_i which might not be possible with just text guidance [14]. Further, as we use base text framework of Rich-Text, we also can specify font size attribute to \mathbf{a}_i^f to control the relative importance of each part in the object.

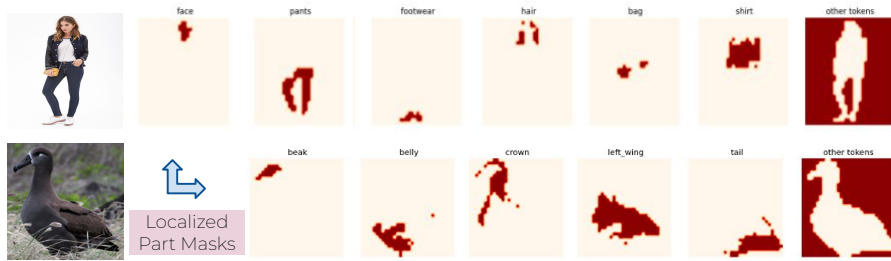


Fig. 4: Segmentation masks for the parts which are localized by Part Diffusion process, for DeepFashion (above) and CUB200 (below) test dataset images.

Text-Preservation of Other Parts. As we only intend to modify the object \mathbf{o} from the original prompt, we also use the Self-Injection techniques from Plug and Play [35] to maintain the overall structure of the object from base prompt generation. Further, to make sure that our diffusion trajectory follows the same path as the other object tokens, the background region is also blend with base noise generation.

$$x_t = \mathbf{M}_b \odot x_t^{\text{base}} + (1 - \mathbf{M}_b) \odot x_t \quad (8)$$

In our case, the attention maps out of the object Mask \mathcal{M}_o and all the object parts not assigned to any token comprise the \mathbf{M}_b , where we start this blend process at $t = T_{\text{blend}}$. We find this to be very useful in preserving the structure of the other parts of the image, and just generating the described parts in the localized region. We provide an overview of the full process in Fig. 2.

4 Experimental Analysis

4.1 Part Localization evaluation

We first evaluate the part localization module, which is based on the novel idea of denoising only the object region with the part-based diffusion feature.

Implementation Details. We use the StableDiffusion version 2.1 for our experimentation purpose. We use the DDIM Scheduler [31] with 50 steps to generate results for SD2.1 to evaluate the part localization process. As ground truth is not available for the part masks of the generated images, we use test sets of the commonly used DeepFashion [23] and CUB-200 [38] datasets for evaluation. These datasets are the standard datasets used for the evaluation of the unsupervised part segmentation approaches. The DeepFashion dataset contains images along with their part segmentation masks, divided into 14 categories of labels. The CUB200 dataset contains the key point annotations for the 14 key points specified for the bird categories. We provide further details in Supp. Section.

Baselines and Problem Setting. As we operate in the region of Zero-shot Unsupervised Part Segmentation, there exists no previous works that report results in such a challenging setting. Hence, to facilitate some comparison, we provide results for the unsupervised learning approaches. We provide results

Table 1: Comparison to Prior Works for the unsupervised part segmentation task. We follow Unsup-Part [11] for evaluation protocols and baseline results for (K=4) parts.

Method	DeepFashion Dataset				CUB200 Dataset			
	FG-NMI	FG-ARI	NMI	ARI	FG-NMI	FG-ARI	NMI	ARI
Unsupervised Learning								
SCOPS [17]	30.7	27.6	56.6	81.4	39.1	17.9	24.4	7.1
Unsup-Parts [11]	44.8	46.6	68.1	90.6	46.0	21.0	43.5	19.6
DFE [10]	-	-	-	-	32.4	14.3	25.9	12.4
Unsupervised Zero-Shot								
Rich-Text [14]	16.0	5.2	48.3	58.7	3.1	0.3	3.1	0.3
StableDiffusion	12.0	3.5	40.6	70.9	8.0	0.6	3.3	0.6
PartCraft(Ours)	24.7	18.0	48.0	73.4	20.5	9.2	18.5	7.7

for the SCOPS [17], which utilizes the internal features of the VGG model to train a model based on self-supervised loss functions to predict parts robustly across categories. The other stronger self-supervised baseline is Unsup-Parts [11], which uses contrastive loss functions to train a network based on equivariance and other vision properties to cluster the object regions into semantic parts. In addition to this, we also report results for the DFF [10] method on the CUB-200 dataset, as they also operate in the same setting. We want to highlight all these unsupervised approaches to training a neural network on the complete training data to be able to segment parts. In contrast, in comparison, our approach is *training free and operates in a zero-shot fashion*. Hence, the performance metrics of zero-shot approaches are not directly comparable to unsupervised methods.

Zero Shot Unsupervised Part Segmentation. As there is no benchmark to evaluate the part localization for generated images, we use the existing dataset of DeepFashion and CUB200 to obtain our results. To obtain segmentation for each image, we first invert the image into the diffusion latent space using Null-Text Inversion [26] method (see Sec. 5 for ablation). To obtain approximate text prompts for inversion, we make use of the BLIP-V2 [21] captioner provided in Diffusers. After providing the desired image and prompt, the Null-Text inversion provides us with inverted latent and unconditioned time embeddings to reconstruct the image of the dataset. We then construct a StableDiffusion baseline in which, in addition to the prompts, we also append the list of part tokens \mathbf{p} to the prompt. We then use the segmentation algorithm described above in Sec. 3.2 to extract token maps corresponding to the part tokens \mathbf{p}_i . We also evaluate a Rich-Text [14] baseline segmentation algorithm for the same. For the proposed part-denoising approach based on parallel diffusion in PartCraft, we first get the inverted latents and embeddings. Then, we generate a base diffusion process to reconstruct the image and use the Part Diffusion to infill the parts of the image. To very fairly compare the StableDiffusion performance with part-denoising, we keep all things the same except the part diffusion process to get masks. Further across these baselines, we use low classifier guidance to ensure proper reconstruction of the dataset image (See Suppl. for details).

Evaluation Protocol. We use the experimental protocol as used by earlier works [11] to facilitate a right point of comparison with earlier works. We want to point out that in our work, the part name (*e.g.*, beak, etc.) is associated with the localized mask, but the unsupervised approaches produce (K=4) parts without any part names. Hence, to make a fair comparison, we create 4 clusters of parts based on their locality, and finally generate segmentation masks with a maximum of 4 clusters. We provide the exact mapping of the part names to cluster labels in the Suppl. Section. We compare the specifically designed metrics [11] of NMI (Normalized Mutual Information) and ARI (Adjusted Rand Index) of the predicted cluster labels with part masks in the case of DeepFashion and key points in case of the CUB dataset. We report the metrics along with their foreground variables (FG-NMI and FG-ARI) for a detailed comparison.

Results. We tabulate the results for all the baselines in Table 1. We find that our approach, PartCraft, significantly improves over the baselines by ≥ 10 points in NMI and ARI, both across most metrics in the Unsupervised Zero-Shot setting. Further, we find that our methods, NMI and ARI, are meaningfully high and, in some cases, are near to the Unsupervised learning approaches, too. This demonstrates that non-trivial part masks can be generated by harnessing the power of the pre-trained diffusion models, and they can serve as a good initial prior for learning part segmentation approaches by using them as base pre-trained models. We provide a qualitative results for PartCraft, where we observe that PartCraft is able to associate the right part with the correct label (Fig 4). Meanwhile, in the StableDiffusion baseline, the parts often get assigned to the wrong part tokens, which is the cause of degraded performance (See Supp. Section). We also observe that in the case of our algorithm, if the part gets localized based on the max condition defined in the segmentation algorithm, the part mask found is usually in the right region (See Fig. 4 and Suppl. Sec. for more results). This demonstrates the effectiveness of our part segmentation procedure, which often sides with not localizing incorrect objects rather than performing arbitrary assignment mistakes.

4.2 PartCraft Image Generation Evaluation

We now evaluate the object composition ability of the proposed approach, PartCraft, in comparison to the baselines. In this section, we use the base generation model as a StableDiffusion 1.5 model to do a fair comparison with the Rich-Text Baseline. We use the same generation setting of using a PNDM scheduler with 41 steps and suggested classifier guidance of 8.5. We keep all the parameters the same as that of the Rich-Text model to perform a fair comparison.

Baselines. For the task of generating the object image based on part-level details of the specified object, we use the strong baselines of Rich-Text Generation and InstructPix2Pix. The Rich-Text Generation method generates the base image itself, whereas the InstructPix2Pix method requires the base image to be generated by us. Apart from this, we also evaluate the standard StableDiffusion baseline in which we add all the part details in the text prompt itself to generate the desired



Fig. 5: Qualitative Comparison for PartCraft. (above) We provide base prompt ‘a photo of a flamingo’ and part prompt as ‘beak - a pelicans beak’. (below) We generate a photo of a man, with part prompt as ‘black jacket and blue jeans’. We find that other baselines either ignore instruction or change the entire composition of base. On contrary, PartCraft is able to correctly localize part and generate specified details.

image. We compare all these baselines with our proposed method, PartCraft, while ensuring that the base parameters and seed are same for the base image generation. This is done to ensure a fair comparison with baselines, as random seeds often change the generation completely. We defer specific details for the baselines to the Suppl. Section.

Visual Comparison. We provide a visual comparison for the baselines in the case of the a) bird image distinctive part generation and b) human image part generations. Across both cases (Fig. 5), our proposed method, PartCraft, only modifies the desired region of the beak and replaces them with the iconic pelican beak. In comparison, the StableDiffusion baseline modifies the image completely. In the Rich-Text generation, the full region corresponding to the bird gets modified instead of only the specified prompt in base generation. For the editing-based InstructPix2Pix method, we observe that it modifies the base image at a global level and is unable to localize modification to the desired part region (Fig. 5). In general, we observe that PartCraft generated images are novel compositions, that look aesthetic and also follow the part-level instructions.

Quantitative Evaluation. As part-specific generation is fine-grained we perform both automatic and user-study evaluation. We performed a user study by inviting 50 participants (28 responded with a full survey). We evaluate the model by asking questions and evaluating metrics on three orthogonal aspects i.e., a) **Localization** of part generation in comparison to the base image (through LPIPS [42]), b) **Text-Consistency** of generated parts by measuring CLIP similarity of the part detailed text prompt with the generated image and c) **Aesthetic Quality** of the generated image through LAION-5B [30] CLIP Aesthetic scorer. In total, we collect about 3.5k opinions. In Fig. 7, we summarize the results in which we observe that PartCraft is significantly preferred over the other baselines in terms of localized and consistent Part Generation. The automated evaluation

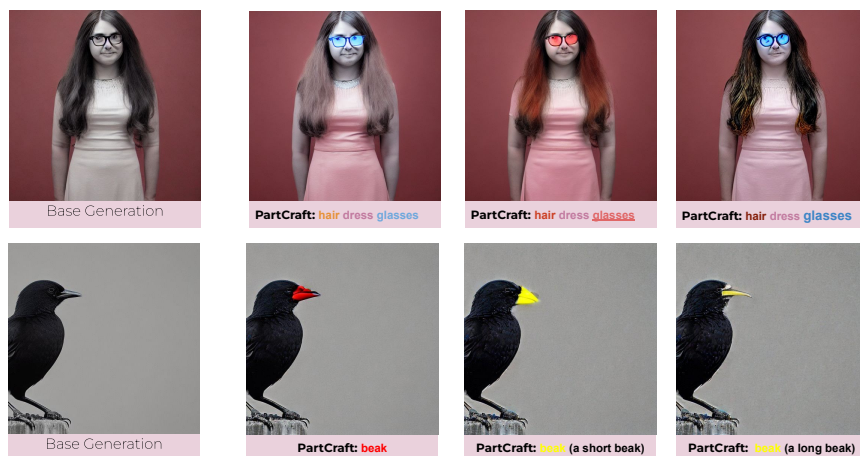
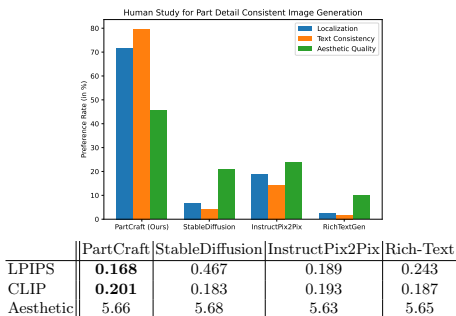


Fig. 6: Attribute Variations for the base generated images are provided for the person portrait, where we change color of hair and eyeglasses, increase weight of eye glasses to change its shape. In the bird example, we generate various colors of beaks and generate its part variations by specifying part description in bracket.

Table 2: Ablation Analysis of PartCraft for Part Localization.

PartCraft (Ablations)		
Method	FG-NMI	FG-ARI
PartCraft	35.4	11.0
w/o Null-Text Inversion	23.1	5.2
w/o Max Localization	21.3	2.8
w/o Dot Product Localization	23.7	5.0
w/o Independent Text	31.2	8.9
PartCraft (Clustering)		
PartCraft (K = 9)	35.4	11.0
PartCraft (K = 4)	20.4	2.8
PartCraft (K = 14)	35.2	10.3

Fig. 7: User Study and Quantitative Results for part-based image generation.



results are provided in the table below which also follow a similar trend as in the user-study, demonstrating effectiveness of PartCraft in localized part generation, while ensuring aesthetics score is similar to that of base model.

5 Analysis and Discussion

Part Diffusion Based Localization. We ablate the components we have introduced in the PartDiffusion process of PartCraft (Sec. 3.2). We provide an analysis of the effect of using **a)** null-text inversion, **b)** max-based localization, **c)** usage of dot product-based protocol in the part assignment, and **d)** independent text embeddings. We have used a subset of CUB-200 images to perform all evaluations, which is kept fixed across ablations. We tabulate the ablations in



Fig. 8: PartCraft generalizes over domains as shown by Claude Monet’s painting image (above), where we specify the dress part of women to follow styles like Van Gogh and Ukiyo-e in different colors. We perform similar modifications to Woody’s image as well, where it’s able to generate aesthetic novel compositions with specified parts.

Table 2. We observe that all components introduced in PartCraft significantly contribute to the overall segmentation performance of the part localization.

Generalization of PartCraft. In Fig. 8, we first have a painting of Claude Monet which is generated by the base StableDiffusion method. We then use PartCraft to specify the dress part of women’s token in the prompt, to dark green color in Monet Style, orange color dress in Van Gogh Style (middle), and green colored dress in Ukiyo-e style. In Fig. 8, we provide edits for the ‘Woody’ character from Toy Story. Across these results, we find that PartCraft is able to generate variations of shirt, pant, and dress colors and is able to generate aesthetic combinations. This zero-shot generalization across domains demonstrates the potential of creative activities that can be enabled with PartCraft.

Limitations: We find that the generation of part is bottlenecked with the part understanding of StableDiffusion. We find that if the part is localized correctly, the text-2-image model is able to generate specified details in PartCraft. Hence, improving part-level localization of these models is a good direction for future.

6 Conclusion

In this work, we introduce PartCraft a method to generate object images with fine-grained details specified at the object part level, using an expressive Rich-Text interface. The PartCraft method introduces a novel part diffusion process, which is responsible for denoising objects using the part features, and then utilizes a region-specific diffusion process to generate part details and compose the final image. PartCraft enables the training-free part-level control for models.

Supplementary Material: Crafting Parts for Expressive Object Composition

Harsh Rangwani^{1,2}, Aishwarya Agarwal², Kuldeep Kulkarni², R. Venkatesh Babu¹, and Srikrishna Karanam²

¹ Indian Institute of Science

² Adobe Research, Bengaluru India

harshr@iisc.ac.in

A Notations

We provide notations used in the paper in Table A.1.

Table A.1: Notation Table

Symbol	Meaning
\mathcal{M}_o	Mask of Object \mathbf{o}
$\hat{\mathbf{b}}, \hat{b}$	Set of Base Prompt Tokens
$\hat{\mathbf{p}}$	Set of Part Prompt Tokens
T_{th}	Threshold After Which The Part Diffusion Starts
$\hat{\mathbf{M}}_j$	Self Attention Map (j^{th} index)
$\hat{\mathbf{m}}_k$	Cross Attention Maps (for k^{th} token)
$x \cdot y$	Dot Product Between x and y , viewed as vectors
$A \odot B$	Elementwise (Hadamard) product between A and B
$\mathbf{M}_{\mathbf{p}_i}$	Part Mask for the part \mathbf{p}_i
\mathbf{a}_i	Attribute Description of part \mathbf{p}_i
$f(\mathbf{p}_i, \mathbf{a}_i)$	Text Description of part \mathbf{p}_i with attributes \mathbf{a}_i
x_t	Partial Denoised Image at time t
ϵ_t	Noise output for estimated noise at time t
D	Denoising U-Net
\mathbf{M}_b	Background (Other) Token Mask
α	Hyperparameter for the Part Diffusion Contribution
δ	Hyperparameter for Part Selection
ϵ	Hyperparameter for the Object Categorization to Background

Table C.1: Part Names in Clusters for CUB and DeepFashion Datasets

Cluster	CUB Part Names	DeepFashion Part Names
0	background	background
1	beak, forehead, left eye, right eye	cap, hair
2	breast, crown, nape, throat	dress, shirt (top) , accessories, outer
3	belly, left leg, right leg, tail	glasses, face, body
4	back, left wing, right wing	pants, footwear, leggings

B Potential Negative Impact

Text-2-image generative models have shown great promise in image generation and can be utilized in content and media creation. However, ensuring the created content is unbiased, harmless, and free of misinformation is essential. Our work gives users more control over text-2-image generation, which should be used responsibly to avoid misinformation.

C Implementation Details

We discuss implementing the two parts of the PartCraft Process, the Part Localization and Part Generation processes.

Part Localization. In Part Localization, we first discuss the implementation on StableDiffusion 2.1, where we use 50 steps of DDIM Scheduler [31] for denoising. As we aim to evaluate our method on CUB-200 and DeepFashion datasets, we first perform inversion using Null-Text Inversion [26] with a guidance scale of 0.05 (other hyper-parameters are kept default). We keep the α value linearly scaled with time steps from 0 to 0.5. To obtain the mask for each segment, we keep a low $\epsilon = 0.05$ threshold, as here, we want to segment the region in all possible parts as the DeepFashion and CUB-200 generate localization masks for the 14 part regions. However, for comparison with baselines producing segments in 4 parts, we perform the following clustering of parts in the four cluster regions (Table C.1). We use (K=9) to cluster the different regions into 4 clusters. We use the foreground masks for objects provided by Choudhury *et al.* [11]³ for evaluating the FG-NMI and FG-ARI metrics in Table 1.

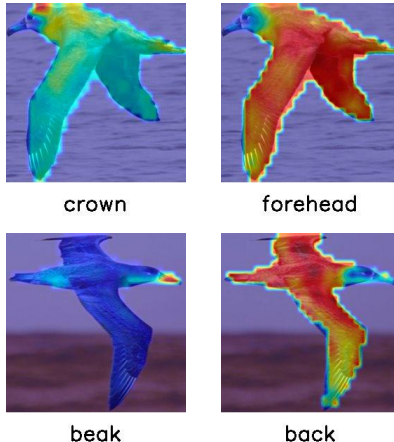
We use StableDiffusion 1.5 to compare the generation results to the Rich-Text [14]⁴ baseline. In this case, we want to start the localization process at a later stage of denoising, as we aimed the part diffusion not to alter the base generation too much; hence, start part denoising from step $T_{th} = 24$. We keep $\epsilon = 0.5$ as the threshold and $\delta = 0.3$ for max part localization (in Eq. 6 and 4) respectively. We use a PNDM scheduler with 41 steps and an 8.5 guidance scale, as done by default in Rich-Text [14] generation.

³ <https://github.com/subhc/unsup-parts>

⁴ <https://github.com/SongweiGe/rich-text-to-image>

Table C.2: Ablation Analysis of PartCraft for Part Localization.

PartCraft (Ablations)		
Method	FG-NMI	FG-ARI
PartCraft	35.4	11.0
w/o Null-Text Inversion	23.1	5.2
w/o Max Localization	21.3	2.8
w/o Dot Product Localization	23.7	5.0
w/o Independent Text	31.2	8.9
PartCraft (Clustering)		
PartCraft (K = 9)	35.4	11.0
PartCraft (K = 4)	20.4	2.8
PartCraft (K = 14)	35.2	10.3

Fig. C.1: Normalized Attention Maps for parts which are localized (left) and non-localized (right).

Part Generation. we use the same scheduler and guidance scale for the part generation. We blend the base x_t^{base} and part generations x_t for 0.2 fraction of the time steps in the denoising process.

Baselines. For the Rich-Text baseline, we use the attribute properties \mathbf{a}_i for the part token and add it to the base token if the part token is present in the base prompt. In other cases, we add the Part information as the footnote of the object token in the base prompt. For the InstructPix2Pix [7] baseline, we individually add the instructions to each part on the base prompt generation through stable diffusion. For the StableDiffusion baseline, we add the PartCraft instructions as the object’s description in the prompt. We use the same StableDiffusion model with the same seed and guidance scale across baselines. We run it on the same Nvidia A100 40GB to ensure the sanity of comparison across methods.

D Analysis of PartCraft

In this section, we provide additional analysis regarding the design choices made in PartCraft. In particular, we ablate the components we have introduced in the PartDiffusion process of PartCraft (Sec. 3.2). We provide an analysis of the effect of using **a)** independent text embeddings, **b)** usage of dot product-based protocol in the part assignment, and **c)** the visualization of attention maps for the localized and unlocalized parts. We have used a subset of CUB-200 images to perform all evaluations, which is kept fixed across ablations. We tabulate the ablations in Table C.2 (also including ablations from the main text Table 2) and provide visual results in Fig. C.1. We observe that all components introduced in PartCraft significantly contribute to the overall segmentation performance of the part localization module. Further, in Fig. C.1, we find that if we normalize parts that do not satisfy localization conditions (forehead and back), it leads to



Fig. D.1: Qualitative Comparison of part masks (on DeepFashion) generated from the Stable Diffusion Baseline to PartCraft (Ours). The Stable Diffusion Baseline assigns arbitrary part masks to segments, whereas our part marks are consistent to part.

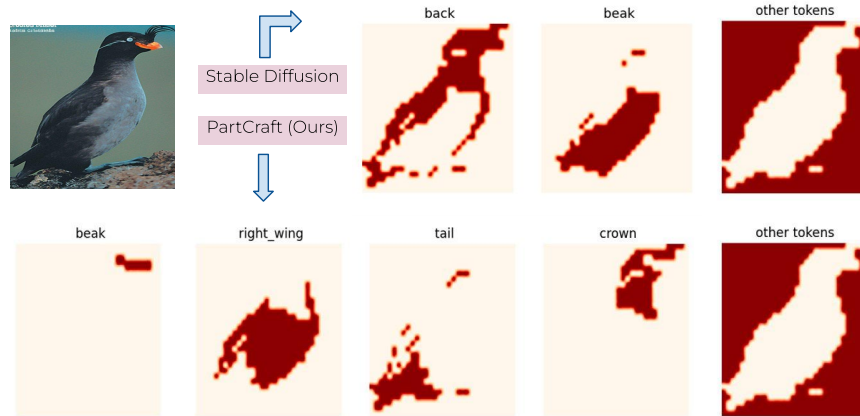


Fig. D.2: Qualitative Comparison of part masks (on CUB200) generated from the Stable Diffusion Baseline to PartCraft (Ours). The Stable Diffusion Baseline assigns arbitrary part masks to segments, whereas our part marks are consistent to part.

high attention values in most regions. This demonstrates the effectiveness of the max-value based selection (Eq. 4) of parts proposed in PartCraft.

For comparison to the Stable Diffusion baseline, in addition to the results provided in Table 1, we provide a qualitative comparison in Fig. D.1 and D.2. The Stable Diffusion baseline assigns arbitrary masks to the wrong parts. On the contrary, if PartCraft localizes parts, they are often correctly associated with the right region of the object. This shows the advantage of using part diffusion rather than inducing additional tokens in the base prompt of StableDiffusion.

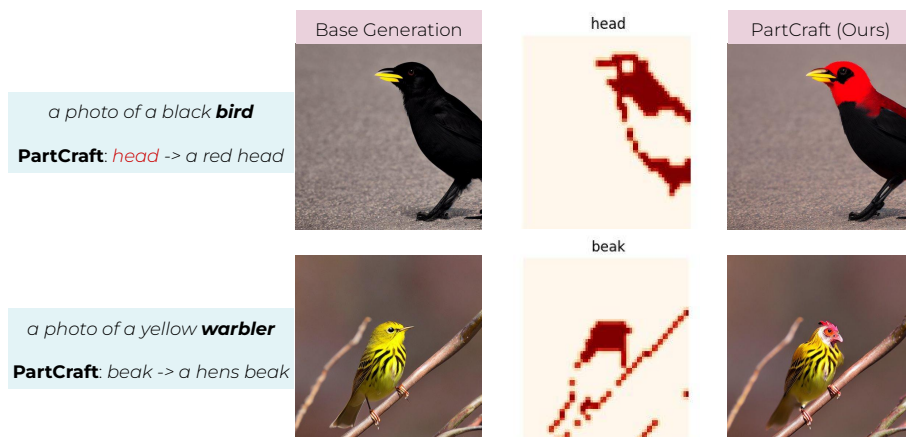


Fig. D.3: PartCraft is robust when the masks don't exactly fit the specified parts. This is because the text description for the masked region contains a description only of specified parts (*e.g.* beak and head above). Hence, the other regions, despite being in the masked region, remain similar to the base generation.

E Qualitative Analysis of PartCraft Generations

Robustnes of PartCraft w.r.t. Masks. PartCraft uses masked diffusion process to generate and compose the object parts. Hence, we first see the effect of the mask region, where we observe (Fig. D.3) that in cases where the mask occupies more region than the desired part, the part diffusion process mostly modifies the requested part. This demonstrates that PartCraft can still generate desired aesthetic outputs in case the masks are not very accurate.

Comparison of PartCraft to Baselines (Fig. 1). In Fig. D.4, we demonstrate a comparison of the StableDiffusion, InstructPix2Pix, and Rich-Text on the prompts demonstrated in the teaser figure. For Rich-Text, we add the description in PartText to the part token if it's present in the base prompt; if not, we add the part description as a footnote in the object token in the base prompt. For InstructPix2Pix, we make instructions regarding part modification one by one on the base generation. We find that the baselines significantly change the entire composition of the object instead of just specified parts.

Limitations. We find that the color guidance applies to the entire masked region. Hence, in some cases, the font color specification \mathbf{a}_c , can alter other areas in minor ways besides the specified part. This is due to color gradient loss, also used in Rich-Text [14] to specify the specific color of the region. We highlight that in the example in Fig. D.5, where some part of the orange lines appear in the shorts worn by the child as it was also the part of mask.



Fig. D.4: Comparison of PartCraft to Other Approaches, for generating using the prompts specified in Fig. 1 of main draft. The PartCraft Approach can modify base generations in the parts specified and can generate aesthetic images in comparison to the state-of-the-art baselines.

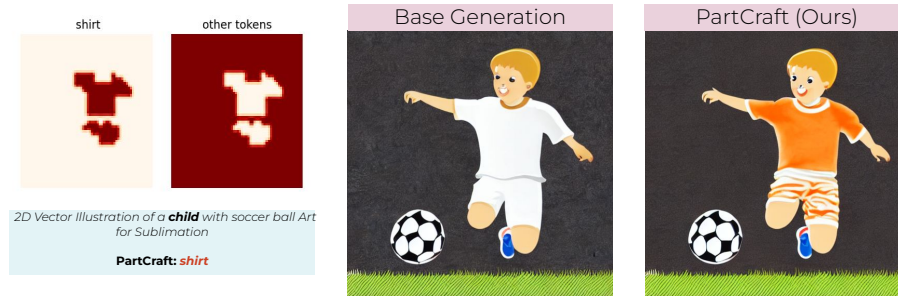


Fig. D.5: A limiting case when only color is specified in PartCraft, and the masks cover extraneous regions. In such cases, when only color guidance is applied, it might leak to some other parts instead of the specified part ('shirt'). As color is added through gradient guidance in the entire masked region.

Acknowledgments: Harsh Rangwani is supported by the PMRF Fellowship at Indian Institute of Science. A considerable part of this work was carried out when Harsh Rangwani was an intern at Adobe Research.

References

1. Abdal, R., Zhu, P., Mitra, N.J., Wonka, P.: Labels4free: Unsupervised segmentation using stylegan. In: Proceedings of the IEEE/CVF International Conference on Computer Vision. pp. 13970–13979 (2021)
2. Agarwal, A., Karanam, S., Joseph, K.J., Saxena, A., Goswami, K., Srinivasan, B.V.: A-star: Test-time attention segregation and retention for text-to-image synthesis (2023)
3. Alaluf, Y., Garibi, D., Patashnik, O., Averbuch-Elor, H., Cohen-Or, D.: Cross-image attention for zero-shot appearance transfer. arXiv preprint arXiv:2311.03335 (2023)
4. Bar-Tal, O., Yariv, L., Lipman, Y., Dekel, T.: Multidiffusion: Fusing diffusion paths for controlled image generation (2023)
5. Bhat, S.F., Mitra, N.J., Wonka, P.: Loosecontrol: Lifting controlnet for generalized depth conditioning (2023)
6. Bhattad, A., McKee, D., Hoiem, D., Forsyth, D.: Stylegan knows normal, depth, albedo, and more. *Advances in Neural Information Processing Systems* **36** (2024)
7. Brooks, T., Holynski, A., Efros, A.A.: Instructpix2pix: Learning to follow image editing instructions. In: CVPR (2023)
8. Chefer, H., Alaluf, Y., Vinker, Y., Wolf, L., Cohen-Or, D.: Attend-and-excite: Attention-based semantic guidance for text-to-image diffusion models. *ACM Transactions on Graphics (TOG)* **42**(4), 1–10 (2023)
9. Chen, M., Laina, I., Vedaldi, A.: Training-free layout control with cross-attention guidance. In: Proceedings of the IEEE/CVF Winter Conference on Applications of Computer Vision. pp. 5343–5353 (2024)
10. Choi, J., Kim, T., Kim, C.: Self-ensembling with gan-based data augmentation for domain adaptation in semantic segmentation. In: Proceedings of the IEEE/CVF International Conference on Computer Vision. pp. 6830–6840 (2019)
11. Choudhury, S., Laina, I., Rupprecht, C., Vedaldi, A.: Unsupervised part discovery from contrastive reconstruction. *Advances in Neural Information Processing Systems* **34**, 28104–28118 (2021)
12. Collins, E., Achant, R., Susstrunk, S.: Deep feature factorization for concept discovery. In: Proceedings of the European Conference on Computer Vision (ECCV). pp. 336–352 (2018)
13. Dhariwal, P., Nichol, A.: Diffusion models beat gans on image synthesis. *Advances in neural information processing systems* **34**, 8780–8794 (2021)
14. Ge, S., Park, T., Zhu, J.Y., Huang, J.B.: Expressive text-to-image generation with rich text. In: IEEE International Conference on Computer Vision (ICCV) (2023)
15. Hertz, A., Mokady, R., Tenenbaum, J., Aberman, K., Pritch, Y., Cohen-Or, D.: Prompt-to-prompt image editing with cross attention control. arXiv preprint arXiv:2208.01626 (2022)
16. Ho, J., Chan, W., Saharia, C., Whang, J., Gao, R., Gritsenko, A., Kingma, D.P., Poole, B., Norouzi, M., Fleet, D.J., et al.: Imagen video: High definition video generation with diffusion models. arXiv preprint arXiv:2210.02303 (2022)
17. Hung, W.C., Jampani, V., Liu, S., Molchanov, P., Yang, M.H., Kautz, J.: Scops: Self-supervised co-part segmentation. In: Proceedings of the IEEE/CVF Conference on Computer Vision and Pattern Recognition. pp. 869–878 (2019)
18. Kang, M., Zhu, J.Y., Zhang, R., Park, J., Shechtman, E., Paris, S., Park, T.: Scaling up gans for text-to-image synthesis. In: Proceedings of the IEEE/CVF Conference on Computer Vision and Pattern Recognition. pp. 10124–10134 (2023)

19. Ko, H.K., Park, G., Jeon, H., Jo, J., Kim, J., Seo, J.: Large-scale text-to-image generation models for visual artists' creative works. In: Proceedings of the 28th International Conference on Intelligent User Interfaces. pp. 919–933 (2023)
20. Lazebnik, S., Schmid, C., Ponce, J.: Semi-local affine parts for object recognition. In: Hoppe, A., Barman, S., Ellis, T. (eds.) British Machine Vision Conference, BMVC 2004, Kingston, UK, September 7-9, 2004. Proceedings. pp. 1–10. BMVA Press (2004)
21. Li, J., Li, D., Savarese, S., Hoi, S.: Blip-2: Bootstrapping language-image pre-training with frozen image encoders and large language models. arXiv preprint arXiv:2301.12597 (2023)
22. Li, Y., Liu, H., Wu, Q., Mu, F., Yang, J., Gao, J., Li, C., Lee, Y.J.: Gligen: Open-set grounded text-to-image generation. In: Proceedings of the IEEE/CVF Conference on Computer Vision and Pattern Recognition. pp. 22511–22521 (2023)
23. Liu, Z., Luo, P., Qiu, S., Wang, X., Tang, X.: Deepfashion: Powering robust clothes recognition and retrieval with rich annotations. In: Proceedings of IEEE Conference on Computer Vision and Pattern Recognition (CVPR) (June 2016)
24. Ma, W.D.K., Lewis, J., Kleijn, W.B., Leung, T.: Directed diffusion: Direct control of object placement through attention guidance. arXiv preprint arXiv:2302.13153 (2023)
25. Maji, S., Rahtu, E., Kannala, J., Blaschko, M., Vedaldi, A.: Fine-grained visual classification of aircraft. arXiv preprint arXiv:1306.5151 (2013)
26. Mokady, R., Hertz, A., Aberman, K., Pritch, Y., Cohen-Or, D.: Null-text inversion for editing real images using guided diffusion models. In: Proceedings of the IEEE/CVF Conference on Computer Vision and Pattern Recognition. pp. 6038–6047 (2023)
27. Patashnik, O., Garibi, D., Azuri, I., Averbuch-Elor, H., Cohen-Or, D.: Localizing object-level shape variations with text-to-image diffusion models. In: Proceedings of the IEEE/CVF International Conference on Computer Vision (ICCV) (2023)
28. Ramesh, A., Pavlov, M., Goh, G., Gray, S., Voss, C., Radford, A., Chen, M., Sutskever, I.: Zero-shot text-to-image generation. In: International Conference on Machine Learning. pp. 8821–8831. PMLR (2021)
29. Rombach, R., Blattmann, A., Lorenz, D., Esser, P., Ommer, B.: High-resolution image synthesis with latent diffusion models. In: Proceedings of the IEEE/CVF conference on computer vision and pattern recognition. pp. 10684–10695 (2022)
30. Schuhmann, C., Beaumont, R., Vencu, R., Gordon, C., Wightman, R., Cherti, M., Coombes, T., Katta, A., Mullis, C., Wortsman, M., et al.: Laion-5b: An open large-scale dataset for training next generation image-text models. *Advances in Neural Information Processing Systems* **35**, 25278–25294 (2022)
31. Song, J., Meng, C., Ermon, S.: Denoising diffusion implicit models. arXiv preprint arXiv:2105.05233 (2021)
32. Tang, R., Liu, L., Pandey, A., Jiang, Z., Yang, G., Kumar, K., Stenetorp, P., Lin, J., Ture, F.: What the daam: Interpreting stable diffusion using cross attention. arXiv preprint arXiv:2210.04885 (2022)
33. Tewel, Y., Kaduri, O., Gal, R., Kasten, Y., Wolf, L., Chechik, G., Atzmon, Y.: Training-free consistent text-to-image generation. arXiv preprint arXiv:2402.03286 (2024)
34. Tian, J., Aggarwal, L., Colaco, A., Kira, Z., Gonzalez-Franco, M.: Diffuse, attend, and segment: Unsupervised zero-shot segmentation using stable diffusion. arXiv preprint arXiv:2308.12469 (2023)

35. Tumanyan, N., Geyer, M., Bagon, S., Dekel, T.: Plug-and-play diffusion features for text-driven image-to-image translation. In: Proceedings of the IEEE/CVF Conference on Computer Vision and Pattern Recognition. pp. 1921–1930 (2023)
36. Vedaldi, A., Mahendran, S., Tsogkas, S., Maji, S., Girshick, R., Kannala, J., Rahtu, E., Kokkinos, I., Blaschko, M.B., Weiss, D., Taskar, B., Simonyan, K., Saphra, N., Mohamed, S.: Understanding objects in detail with fine-grained attributes. In: Proceedings of the IEEE Conference on Computer Vision and Pattern Recognition (CVPR) (June 2014)
37. Voynov, A., Chu, Q., Cohen-Or, D., Aberman, K.: *p+*: Extended textual conditioning in text-to-image generation. arXiv preprint arXiv:2303.09522 (2023)
38. Wah, C., Branson, S., Welinder, P., Perona, P., Belongie, S.: Caltech-ucsd birds-200-2011 dataset. Tech. Rep. CNS-TR-2011-001, California Institute of Technology (2011)
39. Xu, J., Liu, S., Vahdat, A., Byeon, W., Wang, X., De Mello, S.: Open-Vocabulary Panoptic Segmentation with Text-to-Image Diffusion Models. arXiv preprint arXiv:2303.04803 (2023)
40. Yu, J., Xu, Y., Koh, J.Y., Luong, T., Baid, G., Wang, Z., Vasudevan, V., Ku, A., Yang, Y., Ayan, B.K., et al.: Scaling autoregressive models for content-rich text-to-image generation. arXiv preprint arXiv:2206.10789 **2**(3), 5 (2022)
41. Zhang, L., Rao, A., Agrawala, M.: Adding conditional control to text-to-image diffusion models. In: Proceedings of the IEEE/CVF International Conference on Computer Vision. pp. 3836–3847 (2023)
42. Zhang, R., Isola, P., Efros, A.A., Shechtman, E., Wang, O.: The unreasonable effectiveness of deep features as a perceptual metric. In: Proceedings of the IEEE conference on computer vision and pattern recognition. pp. 586–595 (2018)